Supplemental Figure Legends

Supplemental Figure 1, Related to Figure 1: Hsc70-4 protein levels in muscle are unchanged upon TDP-43 overexpression in motor neurons. (**A**) Western blot for Hsc70-4 levels in NMJ preparations of TDP-43 expressing larvae. Genotypes as indicated on bottom. Actin was used as a loading control. (**B**) Quantification of Hsc70-4 protein levels from western blots represented as a ratio to D42>w^{1118} controls. (**C**) qPCR for *hsc70-4* mRNA in NMJ preparations of animals expressing TDP-43^{WT} or TDP-43^{G298S} in motor neurons versus controls. (**D-F**) Confocal images of muscle from neuromuscular junctions of third instar larvae immunostained for Hsc70-4. Genotypes and antibodies as indicated on top. Scale bar (D) 10 μm.

Supplemental Figure 2, Related to Figure 3: Hsc70-4 overexpression does not alter TDP-43 protein or mRNA levels. (**A**) Western blot for TDP-43 YFP from whole larval samples. Genotypes as indicated on bottom. Antibodies as indicated on left. Actin was used as a loading control. (**B**) Quantification of TDP-43 levels from western blots represented as a ratio to TDP-43^{WT} and TDP-43^{G298S} alone. (**C**) qPCR for *tdp-43* mRNA in whole larval samples. Genotypes as indicated on bottom.

Supplemental Figure 3, Related to Figure 3: Hsc70-4 but not Hsp83 or Hsc70-3, modulates TDP-43 mediated locomotor dysfunction. (**A**) D42 Gal4 expression of TDP-43^{WT} results in increased larval turning time that is suppressed by overexpression of Hsc70-4^{WT} and enhanced by Hsc70-4^{D10N} and Hsc70-4^{3KA}. (**B**) D42 Gal4 expression of TDP-43^{G298S} results in increased larval turning time that is suppressed by overexpression of Hsc70-4^{WT} and unaltered by Hsc70-4^{D10N} and Hsc70-4^{3KA}. (**C**) D42 Gal4 expression of TDP-43 variants Q331K and M337V results in increased larval turning time that is suppressed by overexpression of Hsc70-4^{WT}. (**A**) D42 Gal4 expression of TDP-43^{WT} and TDP-43^{G298S} results in increased larval turning time that is not altered by overexpression of Hsp83. (**B**) D42 Gal4 expression of TDP-43^{WT} and TDP-43^{G298S} results in locomotor dysfunction that is not altered by overexpression of Hsc70-3.

Supplemental Figure 4, Related to Figure 3: The distribution of the synaptic proteins cysteine string protein and bruchpilot are not altered by motor neuron expression of TDP-43 or upon co-overexpression with Hsc70-4. (**A-F**) Confocal images of neuromuscular junctions from third instar larvae immunostained for Bruchpilot (NC82) and the neuronal membrane marker Hrp. Genotypes as indicated on top and left and antibodies as indicated on top. (**A'-F'**) Confocal images of neuromuscular junctions from third instar larvae immunostained for Bruchpilot (NC82). Genotypes as indicated on top and left and antibodies as indicated on top. (**G**) Quantification of active zones (NC82 spots) normalized to bouton area. (**H**) Quantification of active zone intensity normalized to NC82 area and the number of NC82 spots. (**I-N**) Confocal images of neuromuscular junctions from third instar larvae immunostained for Cysteine String Protein (Csp) and the neuronal membrane marker Hrp. Genotypes as indicated on top and left and antibodies as indicated on top. (**I'-N'**) Confocal images of neuromuscular junctions from third instar larvae immunostained for Cysteine String Protein (Csp). Genotypes as indicated on top and left and antibodies as indicated on top. (**O**) Quantification of Csp area normalized to bouton area. (**P**) Quantification of Csp intensity normalized to Csp area and bouton area. (**Q**) Quantification of bouton number normalized to muscle area. (**R**) Quantification of bouton area. Scale bars (A, I) 3 μm.

Supplemental Figure 5, Related to Figure 3: TDP-43 expression does not affect FM1-43 dye unloading and Hsc70-4 co-expression restores Hsc70-4 protein levels at the NMJ. (**A-I**) Confocal images of FM1-43 dye remaining in synaptic boutons after 10 min of stimulation in HL-3 saline containing 90 mM KCl and 2 mM Ca^{2+}. Genotypes as indicated on top and left. (**J**) Western blot for Hsc70-4 levels in NMJ preparations. Genotypes as indicated on bottom. Actin was used as a loading control. (**K)** Quantification of Hsc70-4 protein levels from western blots represented as a ratio to D42>w^{1118} controls. Scale bar (A) 10 μm.

Supplemental Figure 6, Related to Figure 4: Other genes involved in the synaptic vesicle cycle are not present in TDP-43 complexes and their distribution is unaltered in RNP and polysome fractions. (**A**) qPCR for *cysteine string protein* (*csp*) mRNA in immunoprecipitated TDP-43 complexes. (**B-D**) *csp* mRNA in input (**B**), RNP (**C**), and polysome (**D**) fractions. (**E**) qPCR for *shibire* (dynamin) mRNA in immunoprecipitated TDP-43 complexes. (**F-H**) *shibire* mRNA in input (**F**), RNP (**G**), and polysome (**H**) fractions. (**I**) qPCR for *auxilin* mRNA in immunoprecipitated TDP-43 complexes. (**J-L**) *auxilin* mRNA in input (**J**), RNP (**K**), and polysome (**L**) fractions.

Supplemental Figure 7, Related to Experimental Procedures: HSPA8 mRNA is bound by endogenous TDP-43 in mouse brains and human cells. (A) RNA seq data reanalyzed from Polymenidou et al (mouse brains). **(B)** RNA seq data reanalyzed from Van Nostrand et al, 2016 (human K562 cells). Conserved regions as indicated.

Supplemental Experimental Procedures

Drosophila Genetics

Transgenic flies expressing human TDP-43 variants with C-terminal YFP tags were generated as previously described (Estes et al., 2011; Estes et al., 2013). Untagged human TDP-43^{WT} was obtained from J. Paul Taylor (Ritson et al., 2010) and untagged human TDP-43^{G298S} was obtained from Takeshi Iwatsubo (Ihara et al., 2013). TDP-43^{Q331K} and TDP-43^{M337V} variants were obtained from Fen-Biao Gao (Lu et al., 2009). The Gal4 driver used was the motor neuron driver D42 Gal4 (Brand and Perrimon, 1993; Gustafson and Boulianne, 1996). For controls, w^{1118}, y1 w67c23; P{Cary}attP40 (Norbert Perrimon), or y'v'; P{caryP} attP40 (Bloomington Drosophila Stock Center) were crossed with the appropriate Gal4 driver. The following stocks were used to manipulate Hsc70-4: w;UAS Hsc70-4 (Konrad Zinsmaier, University of Arizona), UAS Hsc70-4^{WT}, UAS Hsc70-4^{D10N}, and UAS Hsc70-4^{3KA} (Uytterhoeven et al., 2015). To manipulate cysteine string protein w^{1118}, P[14-201.1];Csp^{x1} (Zinsmaier et al., 1994) and w;UAS Csp^{H45Q} (Bronk et al., 2005) were used. Auxilin was manipulated with y[1]v[1];P{y[+t7.7]v[+t1.8]=TRiP.HMS01935}attp40 (Bloomington Drosophila Stock Center) and UAS dAux RFP. Dynamin was overexpressed with w-;;UAS shi WT TF ID115.5. y[1]w[*];Pbac{y[+mDint2]w[+mC]=UAS-Hsp83.Z}VK00033 (Bloomington Drosophila Stock Center) was used to overexpress Hsp83 and w[126];P{w[+mC]=UAS-Hsc70-3.WT}B (Bloomington Drosophila Stock Center) was used to overexpress Hsc70-3. The following C9ORF72 transgenic lines were used: w(Kanai et al.); P{{y[+t7.7] w[+mC]=UAS-GGGGCC.3}attP40 and w(Kanai et al.); P{{y[+t7.7] w[+mC]=UAS-GGGGCC.36}attP40 (Bloomington Drosophila Stock Center).

Electrophysiology

Dissections were made in a modified Ca2 -free HL-3 solution (Stewart et al., 1994). The composition was as follows (in mM): 70 NaCl, 5 KCl, 4 MgCl2, 10 NaHCO3, 5 trehalose, 5 HEPES, and 115 sucrose. For recordings, HL-3 solution was supplemented with 0.6 mM CaCl2 and continuously superfused over the preparation. To elicit a postsynaptic response, the segmental nerve was stimulated for 0.1 ms at 2-3 times the stimulus amplitude required for a threshold response. Voltage signals were amplified with an Axoclamp 2B amplifier (Axon Instruments, Foster City, CA), filtered at 1 kHz, and digitized at 5 kHz directly to disk with a DigiData 1200 interface and pClamp 8.0 software (Axon Instruments). Evoked responses were analyzed with Clampfit 8.0 software (Axon Instruments), and spontaneous events were analyzed with the Mini Analysis Program (Synaptosoft, Leonia, NJ). At least 6 animals per genotype were used for analysis.

FM1-43 Dye Uptake Assays

Wandering third-instar larvae were filleted in Ca^{2+} free HL-3 saline and pinned out on Sylgard dishes. After dissection, larval fillets were briefly washed with Ca^{2+} free HL-3 saline and the anterior pin was relaxed. Larvae were then stimulated for 5 minutes in HL-3 saline containing 4 μ M FM1-43FX, 90 mM KCl, and 2 mM Ca^{2+}. Following stimulation, larvae were extensively washed in Ca^{2+} free HL-3 saline and imaged using a Zeiss LSM 880 confocal microscope. Following dye uptake imaging, larvae were subsequently stimulated for 10 minutes in HL-3 saline containing 90 mM KCl and 2 mM Ca^{2+}. Larvae were again extensively washed in Ca^{2+} free HL-3 saline and imaged using a Zeiss LSM 880 confocal microscope. NIH Image J software was used to calculate FM1-43 dye uptake area and dye intensity. FM1-43 dye uptake area was used for normalization. 24 NMJs from 12 animals per genotype were used for analysis.

Cellular Fractionations and Western Blotting

25 wandering third-instar larvae or 25 7 day old adult males were homogenized in 200 µL low-salt buffer (LS) (10 mM Tris, 5 mM EDTA, 10% sucrose, pH 7.5). Homogenates were briefly centrifuged at 2000 x *g* for 30 seconds. Fat and cuticle were discarded and 100 µL homogenate was kept as input. The remaining 100 µL homogenate was centrifuged at 25,000 x *g* for 30 min. The supernatant represents the LS fraction. The pellet was further extracted with 100 µL ionic detergent containing buffer (Sark) (10 mM Tris, 5mM EDTA, 1% sarkosyl, 10% sucrose, pH 7.5) and 180,000 x *g* for 20 min. The supernatant represents the Sark fraction. The remaining detergent insoluble pellet was solubilized in 100 µL urea containing buffer (Urea) (30 mM Tris, 7M urea, 2M thiourea, 4% CHAPS, pH 8.5). All buffers contained 7X complete protease inhibitor cocktail (Roche) supplemented with 0.5 mM PMSF to block proteolysis. Protein concentrations were calculated using Qubit (Invitrogen). Western blots were performed as

previously described (Coyne et al., 2014; Coyne et al., 2015). 2X Laemmli buffer was added to individual fractions, and 20 µg of protein for each sample was resolved on 4-20% SDS-PAGE precast gradient gels (BioRad) and then transferred to a nitrocellulose membrane (BioRad) for Western blotting. The following primary antibodies were used: 1:6000 rabbit anti-GFP (Invitrogen), and 1:3000 rabbit anti-Hsc70-4 (Konrad Zinsmaier). The secondary antibody was 1:1000 goat anti-rabbit-conjugated-HRP (Thermo Scientific). Proteins were detected using SuperSignal West Femto Substrate (Thermo Scientific) and signal spanning the entire lane was quantified using NIH Image J software. TDP-43 or Hsc70-4 levels in individual fractions were normalized to input. Fisher's exact test was used to determine statistical significance. Experiments were repeated in triplicate.
RNA Solubility Fractionations: A modified cellular fractionation protocol was used. 10 wandering third-instar larvae or were homogenized in 100 µL low-salt buffer (LS) (10 mM Tris, 5 mM EDTA, 10% sucrose, pH 7.5). Homogenates were briefly centrifuged at 2000 x *g* for 30 seconds. Fat and cuticle were discarded and 25 µL homogenate was kept on ice as input. The remaining 75 µL homogenate was centrifuged at 25,000 x *g* for 30 min. The supernatant represents the soluble fraction. The remaining pellet was solubilized in 75 µL urea containing buffer (30 mM Tris, 7M urea, 2M thiourea, 4% CHAPS, pH 8.5) and represents the insoluble fraction. All buffers were made in RNAse free water and contained 7X complete protease inhibitor cocktail (Roche) supplemented with 0.5 mM PMSF to block proteolysis and 40 U/µL RNasin Plus (Promega). Fractions were then prepared for qRT PCR.
Western Blots for Hsc70-4: *Drosophila* NMJ and VNC samples were prepared by filleting wandering third instar larvae in Ca^{2+} free HL-3 saline. Axons were cut just below the ventral nerve cord and retained with the body wall muscles, together comprising the NMJ preparation sample. The ventral nerve cord was collected and used as the VNC sample. Preparations were homogenized in 2X Laemmli buffer. For whole larval samples, larvae were briefly washed in 1X PBS, flash frozen in liquid nitrogen, and then homogenized in 2X Laemmli buffer. All samples were resolved on 4-20% SDS-PAGE gradient gels (BioRad) and transferred on to a nitrocellulose membrane (BioRad). The primary antibodies used were: 1:3000 rabbit anti-Hsc70-4 (Konrad Zinsmaier), and 1:5000 rabbit anti-β Actin (Cell Signaling). The secondary antibodies used were: 1:1000 goat anti-rabbit conjugated HRP (Thermo Scientific), 1:10,000 goat anti-rabbit IRDye 800 (Licor), or 1:10,000 goat anti-rabbit IRDye 680 (Licor). Detection was conducted with SuperSignal West Femto Substrate (Thermo Scientific) or the Licor Odyssey system and quantification performed using NIH Image J software. Experiments were repeated in triplicate.
Western blots for TDP-43: Third instar wandering larvae were briefly washed in 1X PBS, flash frozen in liquid nitrogen, and homogenized in 2X Laemmli buffer and resolved as above. Western blots were conducted as above. The following primary antibodies were used: 1:6000 rabbit anti-GFP (Life Technologies) and 1:5000 rabbit anti-β Actin (Cell Signaling). The secondary antibody used was 1:1000 goat anti-rabbit conjugated HRP (Thermo Scientific). Proteins were detected with SuperSignal West Femto Substrate (Thermo Scientific) and quantification was performed as above. Experiments were repeated in triplicate.

Immunoprecipitations
Adult flies expressing TDP-43^{WT} or TDP-43^{G298S} in motor neurons using the D42 Gal4 driver were collected, frozen, ground into fine powder then resuspended in 3 mL of Lysis buffer (50 mM HEPES pH 7.4, 0.5% Triton X-100, 150 mM NaCl, 30 mM EDTA, 7X Protease Inhibitor Cocktail (Roche), 40 U/µL RNasin Plus (Promega), 0.2 mM (PMSF)). Following homogenization the cell lysate was cleared of debris by centrifugation at 7,000 rpm for 10 min at 4°C. 50 µL of cleared lysate was kept on ice for RNA input and another 50 µL was set aside with 50 µL 2X Laemmli buffer added for protein input. 10 µg of Rabbit α GFP polyclonal antibody (Life Technologies) was added to remaining lysate and incubated for 2 hrs at 4°C. Next, Dynabeads Protein A were added and incubated for 2 hrs at 4°C. 10 µg of Rabbit IgG (Roche) was used as a control. The Dynabeads Protein A immune complexes were washed 3 times for 5 min each in wash buffer (50 mM HEPES pH 7.4, 0.5% Triton X-100, 250 mM NaCl, 30 mM EDTA, 40 U/µL Rnasin Plus). The immune complexes were collected, 50 µL resuspended in 1X Laemmli buffer and analyzed by immunoblotting using standard procedures. The remaining immune complexes (and previously set aside RNA input) were stored at -80°C for later RNA isolation. Protein samples were processed using the western blotting procedure described above. The following primary antibodies were used: 1:10,000 chicken α-GFP (Abcam) and 1:3000 rabbit anti-Hsc70-4 (Konrad Zinsmaier). Secondary antibodies were: 1:10,000 donkey anti-chicken conjugated HRP (Thermo Scientific) and 1:1000 goat anti-rabbit conjugated HRP (Thermo Scientific). Proteins were detected with SuperSignal West Femto Substrate (Thermo Scientific). Experiments were repeated in triplicate.

qRT PCR
RNA Solubility: Following soluble vs insoluble fractionation, RNA was isolated from all fractions (input, soluble, insoluble) using an RNeasy Kit (Qiagen) with on-column DNase treatment. 500 ng RNA was used to perform first strand cDNA synthesis with a Superscript III cDNA synthesis kit (Invitrogen). qPCR reactions were conducted with

SYBR Select Master Mix (Applied Biosystems) and an ABI 7300 Real Time PCR System (Applied Biosystems). Samples were prepared and run in triplicate. The following primers were used: TDP-43 and Hsc70-4 (See Primer Sequences). TDP-43 was used as the reference mRNA and fold change was calculated compared to each respective input using standard ΔΔCT method (Pfaffl, 2001).
Immunoprecipiations: Following RNA immunoprecipitation, RNA was isolated from total lysate, IgG control IP or immunoprecipitated TDP-43 complex using an RNeasy Kit (Qiagen) with on-column DNase treatment. 500 ng RNA was used to perform first strand cDNA synthesis with a Superscript III cDNA synthesis Kit (Invitrogen). qPCR reactions were conducted with SYBR Select Master Mix (Applied Biosystems) and an ABI 7300 Real Time PCR System (Applied Biosystems). Samples were prepared and run in triplicate. The following primers were used: TDP-43, Hsc70-4, Cysteine String Protein, Auxilin, and Dynamin (See Primer Sequences). TDP-43 was used as the reference mRNA as Gpdh is not present in the TDP-43 complex and TDP-43 has previously been shown to bind its own mRNA (Ayala et al., 2011). Fold change was calculated compared to respective input.
Polysome Fractionations: following polysome fractionation, fractions corresponding to the RNP, 40/60S, and 80S peaks were pooled for RNA isolation from the "RNP" or untranslated fraction. RNA from 2+ polysomes was pooled as the "polysome" or actively translating fraction. RNA precipitation was carried out with Trizol (Life Technologies). First strand cDNA synthesis was performed from 500 ng RNA with a Superscript III cDNA synthesis kit (Invitrogen). qPCR reactions were conducted with SYBR select master mix (Applied Biosystems) and an ABI 7300 Real Time PCR System (Applied Biosystems). The following primers were used: Gpdh, Hsc70-4, Cysteine String Protein, Auxilin, and Dynamin (See Primer Sequences). Samples were prepared and run in triplicate. Fractions were normalized to their respective inputs and fold changes were then calculated compared to w^{1118}.
Hsc70-4: NMJ, VNC, and whole larval samples were collected as described above for western blotting procedures. RNA was isolated using an RNeasy Kit (Qiagen) with on-column DNase treatment. 500 ng RNA was used to perform first strand cDNA synthesis with a Superscript III cDNA synthesis Kit (Invitrogen). qPCR reactions were conducted with SYBR Select Master Mix (Applied Biosystems) and an ABI 7300 Real Time PCR System (Applied Biosystems). Samples were prepared and run in triplicate. Primers used were Gpdh and Hsc70-4 (See Primer Sequences). Fold change was calculated compared to w^{1118} controls.
TDP-43: Whole larval samples were prepared as above. RNA isolation, cDNA synthesis, qPCR and analysis were preformed as described above. Primers used were Gpdh and TDP-43 (See Primer Sequences).
iPSC Motor Neurons: 500 ng RNA was used for first strand cDNA synthesis using the RT^2 First Strand Kit (Qiagen). qPCR reactions were performed using TaqMan Fast Advanced Mastermix (Applied Biosystems) on a QuantStudio 6&7 Flex Real-Time PCR System (Applied Biosystems). Primers used were as follows: GAPDH- Assay ID Hs02786624_g1 and HSPA8- Assay ID Hs03044880_gH. GAPDH was used as the reference gene. For TDP-43^{G298S} iPSC qPCR data represent two technical replicates from two differentiations. All other analyses were performed from at least three biological replicates representing at least three different iPSC lines.

Primer Sequences

Gene Name	Primer Sequence
TDP-43	F: ACAACCGAACAGGACCTG
	R: GGCTCATCTTGGCTTTGC
Gpdh	F: CCGCAGTGCTTGTTTTGCT
	R: TATGGCCGAACCCCAGTTG
Hsc70-4	F: CCAGCCAGTTTGATCGAAGG
	R: GCAGGAGCTTTAGACATCTTG
Cysteine String Protein	F: GCAACGATATGCCAACGCATC
	R: ACCATATCTGGCGTGTAAGTGG
Auxilin	F: ATCGCCGAAGCCCAAGATG
	R: GGCGGTATAACTGGAACC
Dynamin	F: CCAGACCAGCTTATCGGAGG
	R: CGAGGTCCGATTTCCCTCAC

Immunohistochemistry and Imaging
Drosophila NMJs: Wandering third instar larvae were filleted in Ca^{2+} free HL-3 saline, pinned out on Sylgard dishes and fixed in 3.5% formaldehyde in PBS, pH 7.2 for 30 minutes, then permeabilized with 0.1% Triton X-100. Blocking agent consisted of 2% BSA and 5% normal goat serum. The following antibodies were used: 1:50 rabbit anti-Hsc70-4 (Konrad Zinsmaier), 1:300 mouse anti-DCSP2 (DSHB), 1:50 mouse anti-Bruchpilot, NC82 (DSHB),

1:500 anti-mouse Alexa 568 (Molecular Probes), 1:500 anti-mouse FITC (Molecular Probes), and 1:200 anti-HRP Cy5 (Molecular Probes) or 1:100 anti-Hrp Alexa 647 (Jackson). 1:300 Phalloidin-488 (Molecular Probes) or 1:300 Rhodamine Phalloidin (Molecular Probes) were used to visualize muscles. Larval muscles 6-7, segment A3 were imaged using a Zeiss LSM 510 or Zeiss 880 confocal microscope. NIH Image J was used for analysis. Hsc70-4 intensity in individual boutons was analyzed in single Z sections (0.38 μM thick). Individual bouton area was defined using Hrp and 65-80 boutons were analyzed per genotype. Hsc70-4 muscle intensity was measured from maximum intensity projections and muscle nuclei were excluded from the analysis. Individual bouton analysis was conducted for the number and intensity of NC82 spots as well as Csp intensity and area. 6-10 randomly selected boutons per NMJ were analyzed and terminal boutons were not used in analysis. Bouton number was assessed by manually counting boutons as defined by Hrp staining in preparations used for NC82 and Csp analysis. For bouton area, each bouton from the above preparations was manually outlined and measured using Hrp staining. 12 NMJs from 6 animals per genotype were used for all analyses.
Mouse NMJs: Wild-type (Jackson Laboratory, 000664, C57Bl/6J) and Prp-TDP-43^{A315T} (Jackson Laboratory, 010700, B6.Cg-Tg (Prnp-TARDBP*A315T)95Balo/J) male mice were euthanized at age P120 and P85, respectively. Mice received food and water *ad libitum*. Prp-TDP-43^{A315T} mice were fed jellified food to mitigate intestinal dysmotility phenotype as recommended by the Jackson Laboratory. All procedures were approved by the University of Kansas Medical Center Institutional Animal Care and Use Committee (IACUC).
Immunohistochemistry experiments we conducted as previously described (Chen et al., 2011; Chen et al., 2012; Nishimune et al., 2004). Mice were fixed by transcardiac perfusion with 2% paraformaldehyde in phosphate-buffered saline (PBS). Muscles were removed and postfixed in the same fixative at room temperature, rinsed in PBS, cryoprotected in 20% sucrose/PBS, frozen in Optimal Cutting Temperature compound (Sakura, Torrence, CA), and cut using a cryostat to obtain 20 μm thick longitudinal sections. Sections were blocked in PBS containing 2% bovine serum albumin, 2% normal goat serum, and 0.1% Triton. Sections were then sequentially incubated with Hsc70/HSPA8 (Abcam 13D3 clone) at 1:1000 overnight at room temperature, washed with PBS, and incubated with a mixture of Alexa Fluor 488-conjugated IgM (Abcam) at 1:1000 and Alexa Fluor 594-conjugated α-bugarotoxin (α-BTX, Invitrogen) at 1:5000 dilution for 2 hours at room temperature. Sections were then washed with PBS and mounted with Vectashield (Vector, Burlingame, CA). No staining was observed when primary antibody was omitted and stained with secondary antibody alone. Epifluorescent images were obtained using a Nikon Eclipse 80i microscope (objective lens: 100 x, numerical aperture 1.49) and analyzed using MetaMorph software (version 7.1.2.0, Molecular Devices). NMJs were visualized using α-BTX to label postsynaptic acetylcholine receptors. To avoid potential complications caused by antibody penetration into the tissue sections, we imaged only *en face* NMJs in the superficial two-thirds of the section and averaged the data from a minimum of 21 NMJs over 6-8 sections for each animal and from 3 animals of each genotype. Quantification regions were defined by manually tracing around areas of α-BTX labeled *en face* NMJs that were in focus. These regions of interest were transferred to Hsc70 images, and mean signal intensity was measured within the region of interest. For representative images shown in figures, Tiff images were cropped and color channels separated using Adobe Photoshop CS6 (Adobe Systems, San Jose, DA). No other adjustments were made to the images.

Primary Neuron Cultures: Transfection, Staining, Image Acquisition, and Analysis
Primary motor neurons from spinal cords of mouse embryos were isolated and plated at day 13.5 (Fallini et al., 2010). Cells were cultured in the glial conditioned medium (Neurobasal, 0.5 mM Glutamax, 2% B27; Invitrogen) supplemented with 2% horse serum (Sigma), and 10 ng/ml each BDNF, CNTF, and GDNF (Peprotech). After 2 days, cells were transfected by magnetofection as previously described (Fallini et al., 2010) with expression plasmids encoding monomeric green fluorescent protein (GFP) fused to human wild-type (WT) and mutant TDP-43 (Q331K, M337V) (Chou et al., 2015). Cells were fixed 24 hrs after transfection. Cells were fixed with 4% paraformaldehyde at room temperature, permeabilized with 0.2% Triton X-100 and blocked with 5% BSA. Mouse anti-Hsc70 and chicken anti-neurofilament antibodies (Abcam) were incubated overnight at 4°C. Cy3- and Cy5-conjugated secondary antibodies (Jackson ImmunoResearch) were incubated for 1 hr at room temperature. Fluorescent imaging was acquired using an epifluorescent microscope (Ti, Nikon) with Z-stack. Image stacks were deconvolved (AutoQuant, Media Cybernetics) and analyzed using ImageJ software (National Institutes of Health). For fluorescent analysis, motor neuron cell bodies and 10μm segments of the axonal growth cones were analyzed. Cell body: GFP (n = 57), TDP-43 WT (n = 49), TDP-43 Q331K (n = 42), TDP-43 M337V (n = 49); Growth cone: GFP (n = 30), TDP-43 WT (n = 24), TDP-43 Q331K (n = 35), TDP-43 M337V (n = 36).

Human iPSC Motor Neuron Differentiation

Control iPSC and C9 iPSC cells (>30 repeats) were differentiated to motor neurons as described by previous studies (Donnelly et al., 2013; Zhang et al., 2015). For demographic information see iPSC Line Demographic Table.

Immunocytochemistry for Hsc70/HSPA8 in iPSC Motor Neurons

Day 55-58 neurons were fixed and immunostained for dendritic marker Map2 (synaptic systems, 1:1500) and Hsc70 (Abcam 1:500). A Zeiss LSM 800 was used to image the cells followed by Imaris imaging software analysis to quantify the average SUM intensity of Hsc70 in dendrites and neuronal cell body. 25-30 cells were analyzed per genotype. For immunocytochemistry in TDP-43 iPSC motor neurons, two control lines and two differentiations of one TDP-43 line were used for analysis. For immunocytochemistry in C9ORF72 iPSC motor neurons, one control and one C9 line were used for analysis.

iPSC Line Demographics

Cell Line	Gender	Age of Biopsy	Diagnosis	C9ORF72 Repeat Length	Figure 6
Control 1	Female	53	Control	<30	Staining and qPCR
Control 2	Male	61	Control	<30	qPCR
Control 3	Male	76	Control	<30	Staining and qPCR
Control 4	Female	35	Control	<30	Staining and qPCR
Control 5	Male	N/A	Control	<30	qPCR
ALS 1	Male	56	C9ORF72 ALS	1150	Staining and qPCR
ALS 2	Male	65	C9ORF72 ALS	>620	qPCR
ALS 3	Male	51	C9ORF72 ALS	>30	qPCR
ALS 4	Male	58	C9ORF72 ALS	>1100	qPCR
ALS 5	Male	Unknown	TDP-43^{G298S}	N/A	Staining and qPCR

Bioinformatics analyses

Mouse sequences for (Polymenidou et al., 2011) were aligned to mm10 using Bowtie2.1.0. eCLIP data for TDP-43 (Van Nostrand et al., 2016) aligned to the human genome hg38 was downloaded from Encode database reference number ENCFFF524PYO. Data was visualized using Integrated Genome Browser, IGV_2.3.93.

Supplemental References

Ayala, Y.M., De Conti, L., Avendano-Vazquez, S.E., Dhir, A., Romano, M., D'Ambrogio, A., Tollervey, J., Ule, J., Baralle, M., Buratti, E.*, et al.* (2011). TDP-43 regulates its mRNA levels through a negative feedback loop. The EMBO journal *30*, 277-288.

Brand, A.H., and Perrimon, N. (1993). Targeted gene expression as a means of altering cell fates and generating dominant phenotypes. Development *118*, 401-415.

Bronk, P., Nie, Z., Klose, M.K., Dawson-Scully, K., Zhang, J., Robertson, R.M., Atwood, H.L., and Zinsmaier, K.E. (2005). The multiple functions of cysteine-string protein analyzed at Drosophila nerve terminals. J Neurosci *25*, 2204-2214.

Chen, J., Billings, S.E., and Nishimune, H. (2011). Calcium channels link the muscle-derived synapse organizer laminin beta2 to Bassoon and CAST/Erc2 to organize presynaptic active zones. J Neurosci *31*, 512-525.

Chen, J., Mizushige, T., and Nishimune, H. (2012). Active zone density is conserved during synaptic growth but impaired in aged mice. J Comp Neurol *520*, 434-452.

Chou, C.C., Alexeeva, O.M., Yamada, S., Pribadi, A., Zhang, Y., Mo, B., Williams, K.R., Zarnescu, D.C., and Rossoll, W. (2015). PABPN1 suppresses TDP-43 toxicity in ALS disease models. Hum Mol Genet *24*, 5154-5173.

Coyne, A.N., Siddegowda, B.B., Estes, P.S., Johannesmeyer, J., Kovalik, T., Daniel, S.G., Pearson, A., Bowser, R., and Zarnescu, D.C. (2014). Futsch/MAP1B mRNA Is a Translational Target of TDP-43 and Is Neuroprotective in a Drosophila Model of Amyotrophic Lateral Sclerosis. J Neurosci *34*, 15962-15974.

Coyne, A.N., Yamada, S.B., Siddegowda, B.B., Estes, P.S., Zaepfel, B.L., Johannesmeyer, J.S., Lockwood, D.B., Pham, L.T., Hart, M.P., Cassel, J.A.*, et al.* (2015). Fragile X protein mitigates TDP-43 toxicity by remodeling RNA granules and restoring translation. Hum Mol Genet *24*, 6886-6898.

Donnelly, C.J., Zhang, P.W., Pham, J.T., Haeusler, A.R., Mistry, N.A., Vidensky, S., Daley, E.L., Poth, E.M., Hoover, B., Fines, D.M.*, et al.* (2013). RNA toxicity from the ALS/FTD C9ORF72 expansion is mitigated by antisense intervention. Neuron *80*, 415-428.

Estes, P.S., Boehringer, A., Zwick, R., Tang, J.E., Grigsby, B., and Zarnescu, D.C. (2011). Wild-type and A315T mutant TDP-43 exert differential neurotoxicity in a Drosophila model of ALS. Human molecular genetics *20*, 2308-2321.
Estes, P.S., Daniel, S.G., McCallum, A.P., Boehringer, A.V., Sukhina, A.S., Zwick, R.A., and Zarnescu, D.C. (2013). Motor neurons and glia exhibit specific individualized responses to TDP-43 expression in a Drosophila model of amyotrophic lateral sclerosis. Disease models & mechanisms *6*, 721-733.
Fallini, C., Bassell, G.J., and Rossoll, W. (2010). High-efficiency transfection of cultured primary motor neurons to study protein localization, trafficking, and function. Mol Neurodegener *5*, 17.
Gustafson, K., and Boulianne, G.L. (1996). Distinct expression patterns detected within individual tissues by the GAL4 enhancer trap technique. Genome *39*, 174-182.
Ihara, R., Matsukawa, K., Nagata, Y., Kunugi, H., Tsuji, S., Chihara, T., Kuranaga, E., Miura, M., Wakabayashi, T., Hashimoto, T.*, et al.* (2013). RNA binding mediates neurotoxicity in the transgenic Drosophila model of TDP-43 proteinopathy. Human molecular genetics *22*, 4474-4484.
Kanai, K., Shibuya, K., and Kuwabara, S. (2011). [Motor axonal excitability properties are strong predictors for survival in amyotrophic lateral sclerosis]. Rinsho shinkeigaku = Clinical neurology *51*, 1118-1119.
Lu, Y., Ferris, J., and Gao, F.B. (2009). Frontotemporal dementia and amyotrophic lateral sclerosis-associated disease protein TDP-43 promotes dendritic branching. Mol Brain *2*, 30.
Nishimune, H., Sanes, J.R., and Carlson, S.S. (2004). A synaptic laminin-calcium channel interaction organizes active zones in motor nerve terminals. Nature *432*, 580-587.
Pfaffl, M.W. (2001). A new mathematical model for relative quantification in real-time RT-PCR. Nucleic acids research *29*, e45.
Polymenidou, M., Lagier-Tourenne, C., Hutt, K.R., Huelga, S.C., Moran, J., Liang, T.Y., Ling, S.C., Sun, E., Wancewicz, E., Mazur, C.*, et al.* (2011). Long pre-mRNA depletion and RNA missplicing contribute to neuronal vulnerability from loss of TDP-43. Nature neuroscience *14*, 459-468.
Ritson, G.P., Custer, S.K., Freibaum, B.D., Guinto, J.B., Geffel, D., Moore, J., Tang, W., Winton, M.J., Neumann, M., Trojanowski, J.Q.*, et al.* (2010). TDP-43 mediates degeneration in a novel Drosophila model of disease caused by mutations in VCP/p97. J Neurosci *30*, 7729-7739.
Stewart, B.A., Atwood, H.L., Renger, J.J., Wang, J., and Wu, C.F. (1994). Improved stability of Drosophila larval neuromuscular preparations in haemolymph-like physiological solutions. Journal of comparative physiology A, Sensory, neural, and behavioral physiology *175*, 179-191.
Uytterhoeven, V., Lauwers, E., Maes, I., Miskiewicz, K., Melo, M.N., Swerts, J., Kuenen, S., Wittocx, R., Corthout, N., Marrink, S.J.*, et al.* (2015). Hsc70-4 Deforms Membranes to Promote Synaptic Protein Turnover by Endosomal Microautophagy. Neuron *88*, 735-748.
Van Nostrand, E.L., Pratt, G.A., Shishkin, A.A., Gelboin-Burkhart, C., Fang, M.Y., Sundararaman, B., Blue, S.M., Nguyen, T.B., Surka, C., Elkins, K.*, et al.* (2016). Robust transcriptome-wide discovery of RNA-binding protein binding sites with enhanced CLIP (eCLIP). Nat Methods *13*, 508-514.
Zhang, K., Donnelly, C.J., Haeusler, A.R., Grima, J.C., Machamer, J.B., Steinwald, P., Daley, E.L., Miller, S.J., Cunningham, K.M., Vidensky, S.*, et al.* (2015). The C9orf72 repeat expansion disrupts nucleocytoplasmic transport. Nature *525*, 56-61.
Zinsmaier, K.E., Eberle, K.K., Buchner, E., Walter, N., and Benzer, S. (1994). Paralysis and early death in cysteine string protein mutants of Drosophila. Science *263*, 977-980.

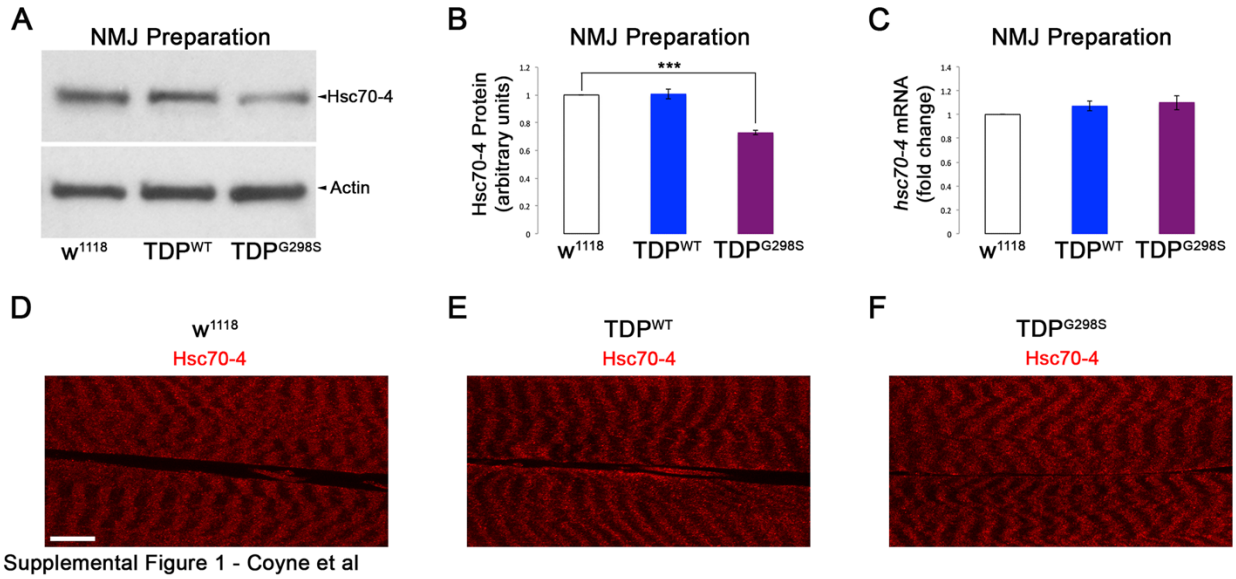

Supplemental Figure 1, Related to Figure 1: Hsc70-4 protein levels in muscle are unchanged upon TDP-43 overexpression in motor neurons. (**A**) Western blot for Hsc70-4 levels in NMJ preparations of TDP-43 expressing larvae. Genotypes as indicated on bottom. Actin was used as a loading control. (**B**) Quantification of Hsc70-4 protein levels from western blots represented as a ratio to D42>w^{1118} controls. (**C**) qPCR for *hsc70-4* mRNA in NMJ preparations of animals expressing TDP-43^{WT} or TDP-43^{G298S} in motor neurons versus controls. (**D-F**) Confocal images of muscle from neuromuscular junctions of third instar larvae immunostained for Hsc70-4. Genotypes and antibodies as indicated on top. Scale bar (D) 10 µm.

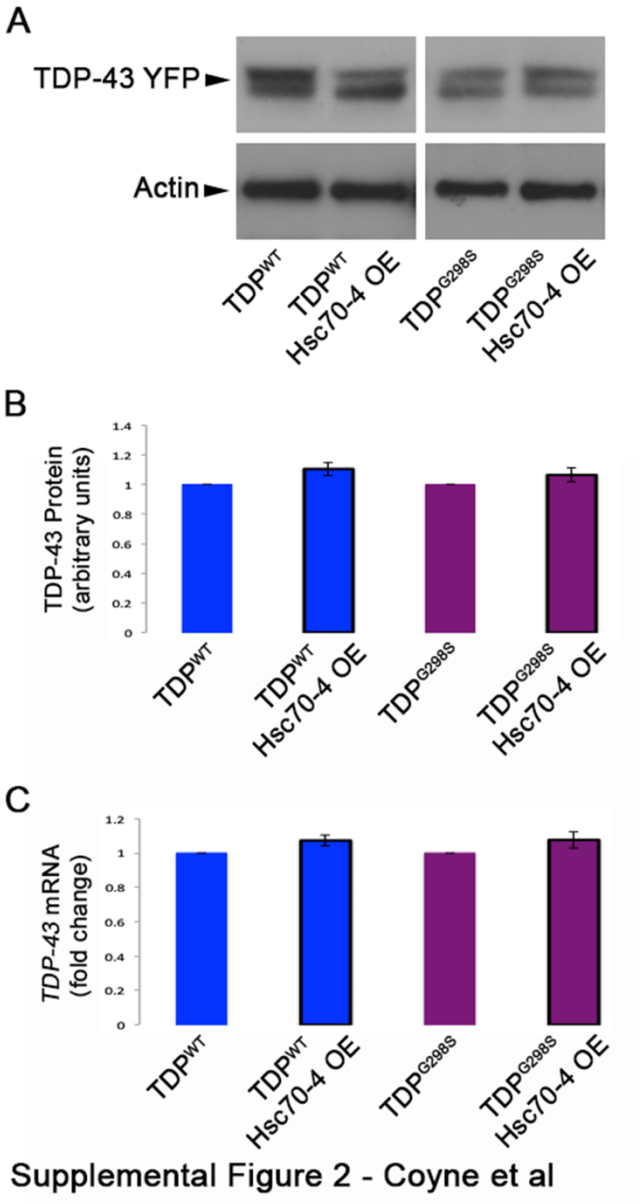

Supplemental Figure 2, Related to Figure 3: Hsc70-4 overexpression does not alter TDP-43 protein or mRNA levels. (**A**) Western blot for TDP-43 YFP from whole larval samples. Genotypes as indicated on bottom. Antibodies as indicated on left. Actin was used as a loading control. (**B**) Quantification of TDP-43 levels from western blots represented as a ratio to TDP-43^{WT} and TDP-43^{G298S} alone. (**C**) qPCR for *tdp-43* mRNA in whole larval samples. Genotypes as indicated on bottom.

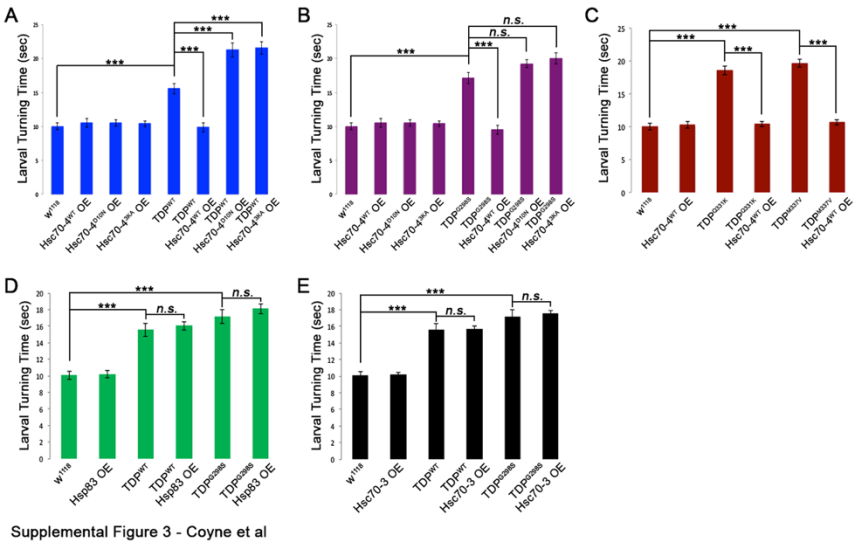

Supplemental Figure 3, Related to Figure 3: Hsc70-4 but not Hsp83 or Hsc70-3, modulates TDP-43 mediated locomotor dysfunction. (**A**) D42 Gal4 expression of TDP-43^{WT} results in increased larval turning time that is suppressed by overexpression of Hsc70-4^{WT} and enhanced by Hsc70-4^{D10N} and Hsc70-4^{3KA}. (**B**) D42 Gal4 expression of TDP-43^{G298S} results in increased larval turning time that is suppressed by overexpression of Hsc70-4^{WT} and unaltered by Hsc70-4^{D10N} and Hsc70-4^{3KA}. (**C**) D42 Gal4 expression of TDP-43 variants Q331K and M337V results in increased larval turning time that is suppressed by overexpression of Hsc70-4^{WT}. (**A**) D42 Gal4 expression of TDP-43^{WT} and TDP-43^{G298S} results in increased larval turning time that is not altered by overexpression of Hsp83. (**B**) D42 Gal4 expression of TDP-43^{WT} and TDP-43^{G298S} results in locomotor dysfunction that is not altered by overexpression of Hsc70-3.

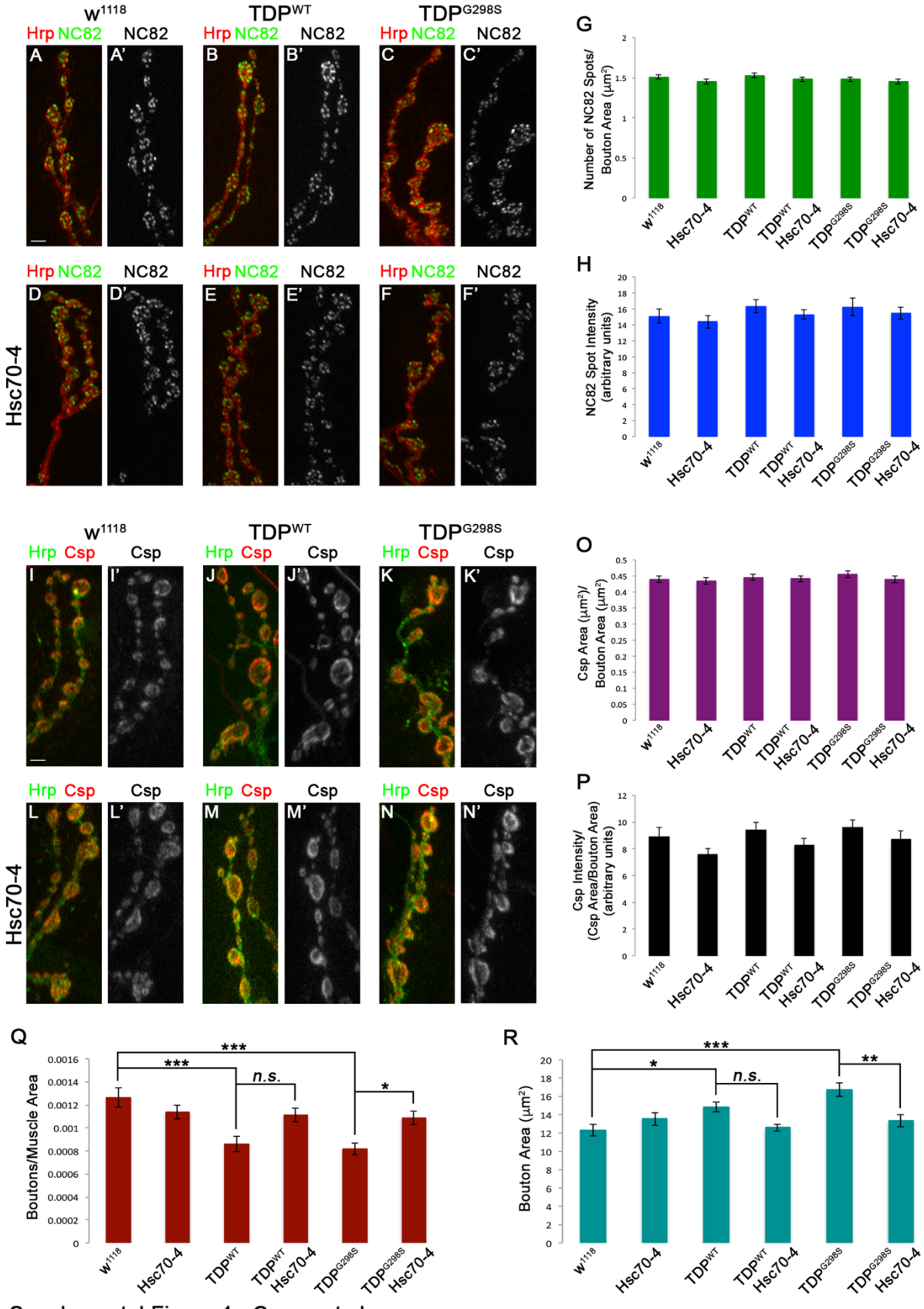

Supplemental Figure 4 - Coyne et al

Supplemental Figure 4, Related to Figure 3: The distribution of the synaptic proteins cysteine string protein and bruchpilot are not altered by motor neuron expression of TDP-43 or upon co-overexpression with Hsc70-4. (**A-F**) Confocal images of neuromuscular junctions from third instar larvae immunostained for Bruchpilot (NC82) and the neuronal membrane marker Hrp. Genotypes as indicated on top and left and antibodies as indicated on top. (**A'-F'**) Confocal images of neuromuscular junctions from third instar larvae immunostained for Bruchpilot (NC82). Genotypes as indicated on top and left and antibodies as indicated on top. (**G**) Quantification of active zones (NC82 spots) normalized to bouton area. (**H**) Quantification of active zone intensity normalized to NC82 area and the number of NC82 spots. (**I-N**) Confocal images of neuromuscular junctions from third instar larvae immunostained for Cysteine String Protein (Csp) and the neuronal membrane marker Hrp. Genotypes as indicated on top and left and antibodies as indicated on top. (**I'-N'**) Confocal images of neuromuscular junctions from third instar larvae immunostained for Cysteine String Protein (Csp). Genotypes as indicated on top and left and antibodies as indicated on top. (**O**) Quantification of Csp area normalized to bouton area. (**P**) Quantification of Csp intensity normalized to Csp area and bouton area. (**Q**) Quantification of bouton number normalized to muscle area. (**R**) Quantification of bouton area. Scale bars (A, I) 3 μm.

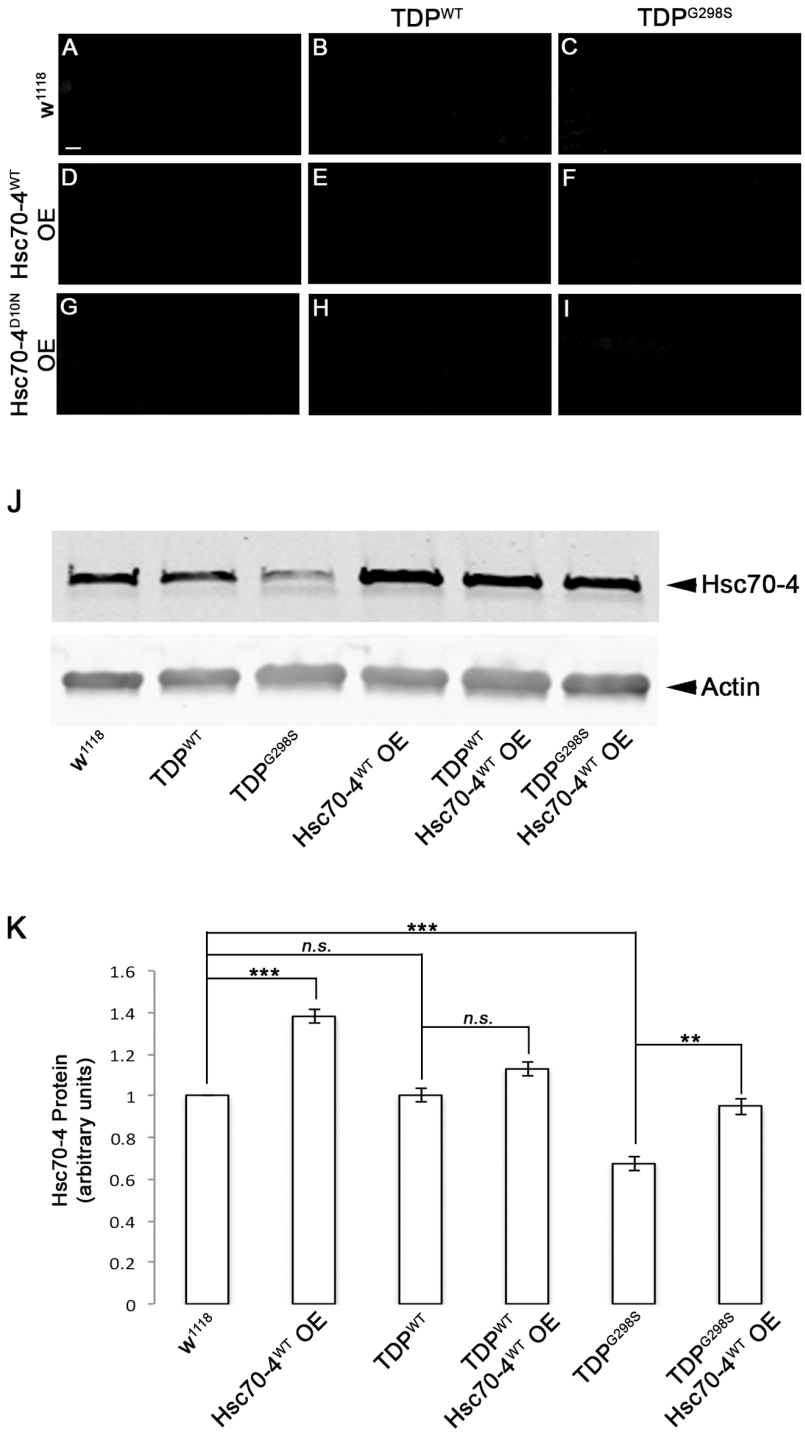

Supplemental Figure 5 - Coyne et al

Supplemental Figure 5, Related to Figure 3: TDP-43 expression does not affect FM1-43 dye unloading and Hsc70-4 co-expression restores Hsc70-4 protein levels at the NMJ. (**A-I**) Confocal images of FM1-43 dye remaining in synaptic boutons after 10 min of stimulation in HL-3 saline containing 90 mM KCl and 2 mM Ca^{2+}. Genotypes as indicated on top and left. (**J**) Western blot for Hsc70-4 levels in NMJ preparations. Genotypes as indicated on bottom. Actin was used as a loading control. (**K)** Quantification of Hsc70-4 protein levels from western blots represented as a ratio to D42>w^{1118} controls. Scale bar (A) 10 μm.

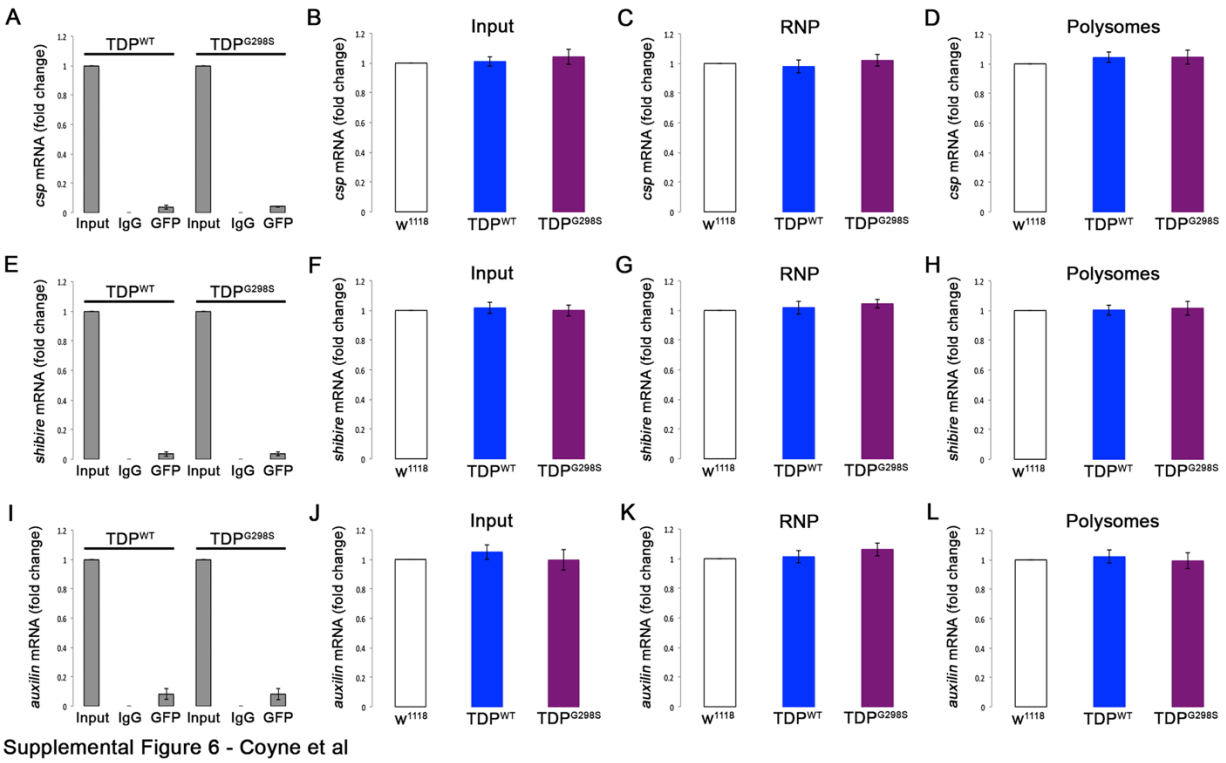

Supplemental Figure 6, Related to Figure 4: Other genes involved in the synaptic vesicle cycle are not present in TDP-43 complexes and their distribution is unaltered in RNP and polysome fractions. (**A**) qPCR for *cysteine string protein* (*csp*) mRNA in immunoprecipitated TDP-43 complexes. (**B-D**) *csp* mRNA in input (**B**), RNP (**C**), and polysome (**D**) fractions. (**E**) qPCR for *shibire* (dynamin) mRNA in immunoprecipitated TDP-43 complexes. (**F-H**) *shibire* mRNA in input (**F**), RNP (**G**), and polysome (**H**) fractions. (**I**) qPCR for *auxilin* mRNA in immunoprecipitated TDP-43 complexes. (**J-L**) *auxilin* mRNA in input (**J**), RNP (**K**), and polysome (**L**) fractions.

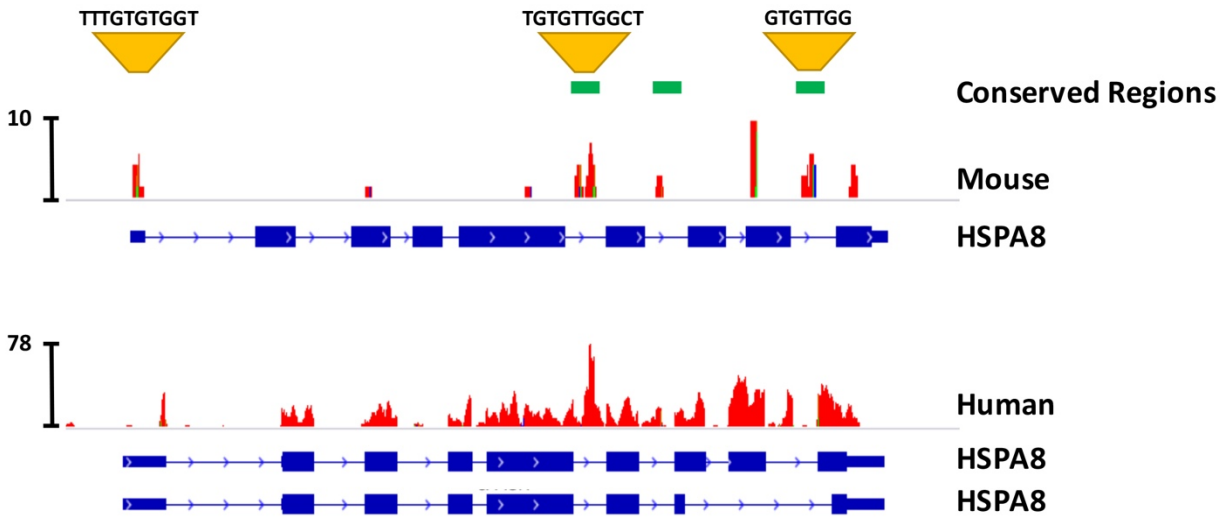

Supplemental Figure 7, Related to Experimental Procedures: HSPA8 mRNA is bound by endogenous TDP-43 in mouse brains and human cells. (A) RNA seq data reanalyzed from Polymenidou et al (mouse brains). **(B)** RNA seq data reanalyzed from Van Nostrand et al, 2016 (human K562 cells). Conserved regions as indicated.